IEEE Access
Multidisciplinary | Rapid Review | Open Access Journal

Received December 18, 2019, accepted January 15, 2020, date of publication January 20, 2020, date of current version February 4, 2020.

Digital Object Identifier 10.1109/ACCESS.2020.2968221

Experimental Comparison of Velocity Observers: A Scissored Pair Control Moment Gyroscope Case Study

STANISLAV ARANOVSKIY[1,4], (Senior Member, IEEE), IGOR RYADCHIKOV[2], EVGENY NIKULCHEV[3], JIAN WANG[4], AND DMITRY SOKOLOV[5]

[1]Equipe Automatique, CentraleSupélec–IETR, 35576 Cesson-Sévigné, France
[2]Laboratory of Robotics and Mechatronics, Kuban State University, Krasnodar 350040, Russia
[3]MIREA–Russian Technological University, Moscow 119454, Russia
[4]School of Automation, Hangzhou Dianzi University, Hangzhou 310018, China
[5]Université de Lorraine, CNRS, Inria, LORIA, 54000 Nancy, France

Corresponding author: Jian Wang (wangjian119@hdu.edu.cn)

This work was supported in part by the Russian Ministry of Education and Science, under Grant 8.2321.2017, and in part by the 111 Project, China, under Grant D17019.

ABSTRACT We consider scissored pair gyroscopes as an auxiliary stabilization system for legged robots. A standard state-feedback control can stabilize the system if all states are available; thus, the velocity estimation becomes the key element for the stabilization. To this end, we implement and experimentally compare a model-free linear differentiator, a model-based full-state linear observer with time-varying gains, and a model-based homogeneous nonlinear differentiator. Moreover, we also show that the considered system cannot be partially linearized via a change of coordinates, and thus is not suitable for a recently reported class of nonlinear observers. The proposed designs are tested on an experimental scissored pair control moment gyroscope setup constructed for a walking robot stabilization.

INDEX TERMS Scissored-pair control moment gyroscope, velocity estimation, differentiator, inverted pendulum, bipedal gait.

I. INTRODUCTION

Bipedal walking robots are one of the fastest rising areas of development and research in robotics. The control must provide various modes of movement in a wide range of enviroment (inclined planes, staircases, obstacles of variable height, wet surface, uneven terrain, non-rigid surface etc.). Even more, the control must take into account the wear of the electromechanical and hydraulic components while maintaining the stability.

Designs of bionic robots try to imitate the knee, the hip joint and other articulations by servomotors. Bionic structures require the reproduction of multiple, including physiologically unexplored psychomotor functions, that stabilize the body during the gait. The complexity of muscle and joint systems creates great structural, dynamic and computational difficulties for the synthesis of control signals. A significant disadvantage of the bionic movements is the difficulty of accounting for nonlinear effects associated with equipment wear, backlash, and changes in friction characteristics. In the existing implementations bionic mechanisms do not provide the required quality of motion / maneuverability. It is important to note that the bionic robotics comes along with the high cost, exceeding practical applications and reasonable manufacturing prices.

In fact, mimicking the nature is equivalent to chasing (inevitable!) mechanical imprecisions: a human's gait is very precise thanks to the quality of his joints. But if he ever tores one of his ligaments, the stability of the articulations is immediately compromised. We do not want to mimic animals completely: at the moment we do not know how to build effective muscles; backlash in artificial joints is almost inevitable.

We want to develop auxiliary stabilization systems that would allow for a better control. For example, by placing a control moment gyroscope ontop for a robot, we would provide an additional support point without touching the rest of the mechanical system. Control moment gyroscope is a

The associate editor coordinating the review of this manuscript and approving it for publication was Tao Wang.

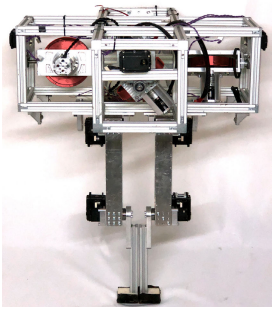

FIGURE 1. We are developing a biped that uses four control moment gyroscopes (highlited in red) as an auxiliary stabilization system.

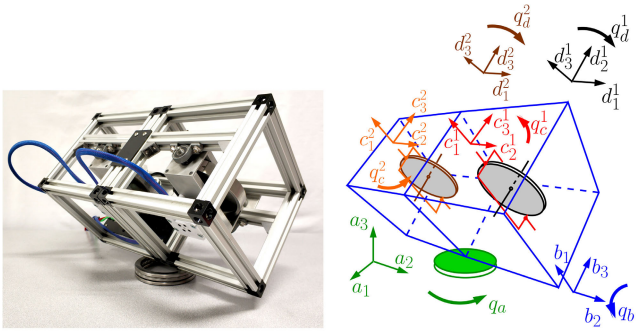

FIGURE 2. Left: inverted pendulum hardware that we study in this paper. The pendulum consists of six bodies: body A (the thrust bearing), body B (the frame), bodies C^1 and C^2 (the single-axis gimbals), and, finally, bodies D^1 and D^2 (the flywheels). Right: corresponding notations. This configuration corresponds to $q_b = -\pi/4$ and $q_c^1 = q_c^2 = \pi/2$.

widely used technological device that uses the reaction of a spinning wheel to external torques. Due to the advantages of a large ratio of produced torque to control torque and relatively low power consumption, CMGs have a wide range of applications, including bicycle stabilization [1], vessel stabilisation [2], motorcycle and robot balancing [3], balancing aid for humans and bipedal exoskeletons [4], [5], attitude steering system for the satellites [6] and underwater vehicles [7].

The research problem of this paper is motivated by the walking robot we are currently developing in the Laboratory of Robotics and Mechatronics of the Kuban State University (refer to Fig. 1). This non-anthropomorphic robot has an auxiliary dynamic stabilization system which consists of two scissored pairs of control moment gyroscopes (CMG). The scissored pairs are orthogonal and thus the problem of vertical stabilization of the robot can be considered for each axis separately. Therefore, stabilization of the robot for one axis can be approximated with a simplified prototype. In this paper we consider such a prototype, namely a scissored pair control moment gyroscope inverted pendulum (Fig. 2). Note that the robot has a modular design: the biped is equipped with four identical CMG cubes.

The key element for stabilization of an inverted pendulum is velocity estimation. Note that our robot uses multiple accelerometers to estimate its tilt angles [8], and we rely on soft sensors for velocity estimation. Velocity estimation for mechanical systems is a well-known problem, and there exist numerous results on observers reconstructing the whole state vector, for both linear and nonlinear systems, see, for example, the recent work by Aranovskiy *et al.* [9] and the references therein for model-based observers and the work [10] for a recent neural-network based observer example. However, a common engineering solution is to consider the velocity estimation problem for each degree of freedom separately rather than to estimate all velocities with a single observer. From the signal processing point of view, this approach can be considered as numerical differentiation, where velocity estimation is seen as online differentiation of a measured position signal, e.g., a first-order difference used in [11]. While differentiator-based velocity observers can be designed model-free, a better performance is typically obtained when observers use (at least partially) available model knowledge: sliding-mode exact differentiators first proposed by Levant in [12], high-gain differentiators as described by Vasiljevic and Khalil in [13], and differentiators proposed by Perruquetti *et al.* [14] that ensure finite-time convergence and robustness with respect to measurement noises and uncertainties. In this paper, we aim at practical comparison of some of the discussed observers.

The contribution of this paper is two-fold: first, we give a rigorous proof that, despite its simplicity, the mechanical system under consideration does not belong to the class of recently reported systems [9], for which a construction of model-based nonlinear observers is known. Next, we propose a comparison of three velocity observers, namely a model-free differentiator, a model-based linear observer and a model-based nonlinear differentiator. All three observers are tested on the hardware we have built for this purpose, and the experimental results are provided.

The preliminary results of this research are reported in [15]. Extending that work, this manuscript presents i) more challenging mechanical system and motion dynamics with the corresponding hardware, ii) the proof that the system does not belong to the class PLvCC [9], iii) the velocity estimation using an observer with time-varying gains, and iv) detailed and extended experimental studies.

The rest of the paper is organized as follows. In section II we present a model of the considered system. Next, in section III we present the state-feedback controller capable to stabilize the system if all states (including velocities) are measured. Then, in section IV we discuss three velocity observers. Hardware experiments and observers comparison are provided in section V. Finally, possible further research directions are discussed in the concluding section VI.

II. MODEL DESCRIPTION

The considered inverted pendulum is shown in Fig. 2. In this paper we follow the notations from the manual of the model 750 control moment gyroscope commercialized by Educational Control Products company [16]. The pendulum consists of six bodies: body A (the thrust bearing, shown in green), body B (the frame, shown in blue),

TABLE 1. Hardware parameters.

Description	Symbol	Value
Total mass, kg	m	2.62
Cube edge length, m	l	0.19
Moments of inertia, kg·m^2:		
of the body B	$[I_b,\ J_b,\ K_b]$	$[10\ 13\ 13]\cdot 10^{-3}$
of the body C	$[I_c,\ J_c,\ K_c]$	$[10\ 2.6\ 9.9]\cdot 10^{-4}$
of the body D	$[I_d,\ J_d,\ K_d]$	$[5.6\ 11\ 5.6]\cdot 10^{-4}$
Disk D velocity, rad/s	ω_d	314
Equilibrium position bias, rad	e	unknown

bodies C^1 and C^2 (the single-axis gimbals, shown in red and orange), and, finally, bodies D^1 and D^2 (the flywheels, shown in brown and black). We associate a basis with each of the bodies: $\{\vec{a}_1, \vec{a}_2, \vec{a}_3\}$, $\{\vec{b}_1, \vec{b}_2, \vec{b}_3\}$, $\{\vec{c}_1^1, \vec{c}_2^1, \vec{c}_3\}$, $\{\vec{c}_1^2, \vec{c}_2^2, \vec{c}_3^2\}$, $\{\vec{d}_1^1, \vec{d}_2^1, \vec{d}_3^1\}$ and $\{\vec{d}_1^2, \vec{d}_2^2, \vec{d}_3^2\}$, respectively. We assume that all the bodies are symmetric; so the inertia matrices are diagonal. Let us denote by $\mathrm{diag}(I_c, J_c, K_c)$ the inertia matrix (w.r.t the center of mass) of the bodies C^1 and C^2; and by $\mathrm{diag}(I_d, J_d, K_d)$ the inertia matrix of the bodies D^1 and D^2. In the same manner, we denote the inertia matrix of the body A as $\mathrm{diag}(I_a, J_a, K_a)$. As for the body B, the frame consists of two identical cubes, and we denote by I_b, J_b and K_b the principal moments of inertia of each half of the frame w.r.t. the center of mass of each cube.

We denote by q_a the angle of rotation between the "north" direction and the body A; the angle of the body B with respect to the vertical is denoted as q_b; the angle of the bodies C^1 and C^2 with respect to the body B are denoted as q_c^1 and q_c^2; and the angle of the bodies D^1 and D^2 with respect to the body C^1 and C^2 are denoted as q_d^1 and q_d^2. The configuration shown in Fig. 2 corresponds to the angles $q_b = -\pi/4$ and $q_c^1 = q_c^2 = \pi/2$. Note that the equilibrium position of an actual robot depends on the configuration of the legs and may be subject to external disturbances; therefore, for our cube we model the equilibrium point as $q_b = -\pi/4 - e$, where e is the unknown (small) bias. The notations and the corresponding hardware parameters are summarized in the Table 1.

With these definitions, the vectors of angular velocities can be found as:[1]

$$\vec{\omega}_a = \begin{bmatrix} 0 \\ 0 \\ \dot{q}_a(t) \end{bmatrix},$$

$$\vec{\omega}_b = \begin{bmatrix} 0 \\ \dot{q}_b(t) \\ 0 \end{bmatrix} + R_{AB}(q_b) \times \vec{\omega}_a,$$

$$\vec{\omega}_c^1 = \begin{bmatrix} \dot{q}_c^1(t) \\ 0 \\ 0 \end{bmatrix} + R_{BC}(q_c^1) \times \vec{\omega}_b,$$

$$\vec{\omega}_d^1 = \begin{bmatrix} 0 \\ \dot{q}_d^1(t) \\ 0 \end{bmatrix} + R_{CD}(q_d^1) \times \vec{\omega}_c^1,$$

[1]When clear from the context, in the sequel the argument of time is omitted.

$$\vec{\omega}_c^2 = \begin{bmatrix} \dot{q}_c^2(t) \\ 0 \\ 0 \end{bmatrix} + R_{BC}(q_c^2) \times \vec{\omega}_b,$$

$$\vec{\omega}_d^2 = \begin{bmatrix} 0 \\ \dot{q}_d^2(t) \\ 0 \end{bmatrix} + R_{CD}(q_d^2) \times \vec{\omega}_c^2.$$

where R_{AB}, R_{BC} and R_{CD} are the transformations between the bases of corresponding bodies:

$$R_{AB}(\alpha) = \begin{bmatrix} \cos\alpha & 0 & -\sin\alpha \\ 0 & 1 & 0 \\ \sin\alpha & 0 & \cos\alpha \end{bmatrix},$$

$$R_{BC}(\alpha) = \begin{bmatrix} 1 & 0 & 0 \\ 0 & \cos\alpha & \sin\alpha \\ 0 & -\sin\alpha & \cos\alpha \end{bmatrix},$$

$$R_{CD}(\alpha) = \begin{bmatrix} \cos\alpha & 0 & -\sin\alpha \\ 0 & 1 & 0 \\ \sin\alpha & 0 & \cos\alpha \end{bmatrix}.$$

Then the parallel axis theorem allows us to write the total kinetic energy of the system as:

$$\begin{aligned} T = \frac{1}{2}\Big(& \vec{\omega}_d^{1\top} \times \mathrm{diag}(I_d, J_d, K_d) \times \vec{\omega}_d^1 \\ & + \vec{\omega}_c^{1\top} \times \mathrm{diag}(I_c, J_c, K_c) \times \vec{\omega}_c^1 \\ & + \vec{\omega}_d^{2\top} \times \mathrm{diag}(I_d, J_d, K_d) \times \vec{\omega}_d^2 \\ & + \vec{\omega}_c^{2\top} \times \mathrm{diag}(I_c, J_c, K_c) \times \vec{\omega}_c^2 \\ & + 2\vec{\omega}_b^{\top} \times \mathrm{diag}\left(I_b, J_b + \frac{1}{2}ml^2, K_b\right) \times \vec{\omega}_b \\ & + \vec{\omega}_a^{\top} \times \mathrm{diag}\left(I_a, J_a, K_a + \frac{1}{2}ml^2\right) \times \vec{\omega}_a \Big). \end{aligned}$$

The potential energy is given by $P = \sqrt{2}mlg\cos(q_b + \pi/4 + e)$. Therefore the Lagrangian can be written as $\mathcal{L} = T - P$. The idea is to apply torques τ_c^1, τ_c^2, τ_d^1 and τ_d^2 to the bodies C^1, C^2, D^1 and D^2, respectively; thus we can find the Euler–Lagrange equations:

$$\begin{cases} \frac{d}{dt}\left(\frac{\partial \mathcal{L}}{\partial \dot{q}_a}\right) - \frac{\partial \mathcal{L}}{\partial q_a} = 0 \\ \frac{d}{dt}\left(\frac{\partial \mathcal{L}}{\partial \dot{q}_b}\right) - \frac{\partial \mathcal{L}}{\partial q_b} = 0 \\ \frac{d}{dt}\left(\frac{\partial \mathcal{L}}{\partial \dot{q}_c^1}\right) - \frac{\partial \mathcal{L}}{\partial q_c^1} = \tau_c^1 \\ \frac{d}{dt}\left(\frac{\partial \mathcal{L}}{\partial \dot{q}_c^2}\right) - \frac{\partial \mathcal{L}}{\partial q_c^2} = \tau_c^2 \\ \frac{d}{dt}\left(\frac{\partial \mathcal{L}}{\partial \dot{q}_d^1}\right) - \frac{\partial \mathcal{L}}{\partial q_d^1} = \tau_d^1 \\ \frac{d}{dt}\left(\frac{\partial \mathcal{L}}{\partial \dot{q}_d^2}\right) - \frac{\partial \mathcal{L}}{\partial q_d^2} = \tau_d^2 \end{cases} \tag{1}$$

These equations are very cumbersome, but we will shortly simplify the system. To this end, we introduce the following hypotheses.

Hypothesis 1: A scissored pair control moment gyroscope implies a symmetric control for the gimbals, the idea behind it is to cancel parasitic impact on the body A. Thus we enforce the following constraints:

$$\tau_d := \tau_d^1 = -\tau_d^2$$
$$\tau_c := \tau_c^1 = -\tau_c^2$$

Hypothesis 2: The initial conditions are also symmetric for the bodies C^1, C^2 and D^1, D^2:

$$q_d^1(0) = q_d^2(0) = 0$$
$$\dot{q}_d^1(0) = \dot{q}_d^2(0) = 0$$
$$q_c^1(0) = q_c^2(0) = \frac{\pi}{2}$$
$$\dot{q}_c^1(0) = \dot{q}_c^2(0) = 0$$

The initial conditions of the body A are $q_a(0) = \dot{q}_a(0) = 0$.

Hypothesis 3: For control moment gyroscope systems, the nominal operation mode assumes $|\dot{q}_d| \gg \max(|\dot{q}_a|, |\dot{q}_b|, |\dot{q}_c|)$, and regulation of the velocity $\dot{q}_d$ is performed by the means of local motor controllers. We assume that these controllers provide fast and accurate velocity regulation ensuring that $\dot{q}_d$ is constant and equals to the nominal velocity, see Table 1, thus $\ddot{q}_d \approx 0$.

The symmetry of the initial conditions and the control introduced in Hypotheses 1 and 2 results in the following symmetry of the signals, allowing us to reduce the cumbersomeness of the equations of motion:

$$q_d^1(t) = -q_d^2(t) =: q_d(t)$$
$$q_c^1(t) = \pi - q_c^2(t) =: q_c(t)$$

Going further, it is easy to see that Hypothesis 1 (symmetric control of the scissored pair) and the initial conditions (Hypothesis 2), imply that the body A is not subject to any torque: $q_a(t) = \dot{q}_a(t) = 0$.

The above assumptions allow to simplify the system (1) and write it down explicitly:

$$\begin{aligned} 0 &= 2\left(J_1 + J_2\cos^2 q_c\right)\dot{\omega}_b - 2J_2\sin(2q_c)\omega_c\omega_b \\ &\quad -2J_d\sin(q_c)\omega_c\omega_d - \sqrt{2}mlg\sin\left(q_b + \frac{\pi}{4} + e\right), \\ \tau_c &= (I_c + I_d)\dot{\omega}_c + J_d\omega_b\omega_d\sin q_c + \frac{1}{2}J_2\sin(2q_c)\omega_b^2, \end{aligned} \quad (2)$$

where $J_1 := I_d + J_b + K_c + \frac{1}{2}ml^2$, $J_2 := J_c - I_d + J_d - K_c$ and $\omega_b(t) := \dot{q}_b(t)$, $\omega_c(t) := \dot{q}_c(t)$, $\omega_d(t) := \dot{q}_d(t)$. In this expression we use the rotational symmetry $K_d = I_d$ of the disk D.

In practice it means that our scissored pair (Fig. 2) can be thought of as a single gimbal 1D inverted pendulum (refer to Fig. 3). If these Hypotheses 1–2 are violated, than the approximation error will appear as un unknown function on the left-hand side of the simplified model (2). However, the experimental studies (Section V) show that the imposed assumptions are reasonable, thus allowing for for satisfactory velocity estimation.

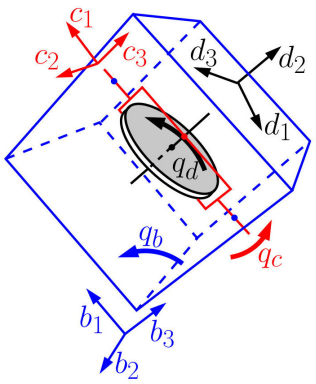

FIGURE 3. A graphic representation of the system 3 with corresponding notations. This configuration corresponds to $q_b = -\pi/4$ and $q_c = \pi/2$.

This simplified system contains only three bodies B, C and D, thus greatly simplifying the analysis. Note that even if the constraints allow us to analyze the 1D pendulum, all the experiments presented in the Section V are performed on the hardware shown in Fig. 2.

Moreover, in our hardware the gimbals C^1 and C^2 are controlled by the means of servo drives that ensure velocity tracking. In this case, the velocity ω_c can be considered as an input signal. Under these assumptions the system (2) can be rewritten as

$$\begin{aligned} \dot{q}_b &= \omega_b, \\ \dot{\omega}_b &= \frac{\omega_c(J_d\omega_d\sin q_c + J_2\omega_b\sin(2q_c))}{J_1 + J_2\cos^2 q_c} \\ &\quad + \frac{\frac{mlg}{\sqrt{2}}\sin\left(q_b + \frac{\pi}{4} + e\right)}{J_1 + J_2\cos^2 q_c}, \\ \dot{q}_c &= \omega_c. \end{aligned} \quad (3)$$

III. LINEARIZATION-BASED STABILIZATION

For the system (3), the desired equilibrium is defined as

$$\Omega_0 := \left\{q_b = -\frac{\pi}{4} - e,\ \omega_b = 0,\ q_c = \frac{\pi}{2}\right\}.$$

In what follows we say that a control law (locally) stabilizes the system (3) if under this control law the point Ω_0 is (locally) attractive.

To proceed, it is convenient to define a new state variable as a deviation of the actual position from the desired equilibrium, $x := \begin{bmatrix} q_b & \omega_b & q_c \end{bmatrix}^\top - \Omega_0$. Then the system (3) can be rewritten as

$$\dot{x} = f(x,u) = \begin{bmatrix} x_2 \\ \frac{u(J_d\omega_d\cos x_3 - J_2\ x_2\sin(2\ x_3)) + \frac{mgl}{\sqrt{2}}\sin x_1}{J_1 + J_2\sin^2\ x_3} \\ u \end{bmatrix}, \quad (4)$$

where $u = \omega_c$.

The state variable x_3 can be computed through the measurements of the signal q_c; however, since the offset e is not known, the signal x_1 can not be computed. Thus, we define

the vector of measurements as

$$y = \begin{bmatrix} q_b + \dfrac{\pi}{4} \\ q_c - \dfrac{\pi}{2} \end{bmatrix} = \begin{bmatrix} x_{1-e} \\ x_3 \end{bmatrix}. \tag{5}$$

Then the control goal is to find a control law that stabilizes (4) at the origin using the measurements y.

A common practice to stabilize a (sufficiently well-behaved) nonlinear system is to linearize the system around the desired equilibrium. For the system (4) such equilibrium is given by $x = 0$, $u = 0$. Let us define

$$A := \frac{\partial f}{\partial x}(0,0) = \begin{bmatrix} 0 & 1 & 0 \\ \dfrac{mgl}{\sqrt{2}J_1} & 0 & 0 \\ 0 & 0 & 0 \end{bmatrix},$$
$$B := \frac{\partial f}{\partial u}(0,0) = \begin{bmatrix} 0 \\ \dfrac{J_d\omega_d}{J_1} \\ 1 \end{bmatrix} \tag{6}$$

Then the linearization of (4) around the origin is given by $\dot{x} = Ax + Bu$.

It is tempting to use the state-feedback static control

$$u := -K \begin{bmatrix} y_1 & x_2 & y_2 \end{bmatrix} = -Kx - k_1 e, \tag{7}$$

where $K := \begin{bmatrix} k_1 & k_2 & k_3 \end{bmatrix}$ is the gain vector.

The problem, however, is that the equilibrium point would be $(A - BK)^{-1} Bk_1 e = \begin{bmatrix} 0 & 0 & -\frac{k_1}{k_3} \end{bmatrix}^\top e$.

Therefore, the stabilization goal $|x| \to 0$ is not achieved under the control law (7). In order to overcome the nonzero steady-state body C angle problem, we add an integral action. To this end, we introduce an auxiliary variable x_e defined as $\dot{x}_e := 0 - x_3$, where zero stays as the reference for x_3. Then the extended state-space model is

$$\begin{bmatrix} \dot{x} \\ \dot{x}_e \end{bmatrix} = \underbrace{\left[\begin{array}{ccc|c} & A & & 0_{3\times 1} \\ \hline 0 & 0 & -1 & 0 \end{array}\right]}_{A_e} \begin{bmatrix} x \\ x_e \end{bmatrix} + \underbrace{\begin{bmatrix} B \\ 0 \end{bmatrix}}_{B_e} u.$$

The pair A_e, B_e is controllable and we can design the extended control law

$$\begin{aligned} u &:= -K_e \begin{bmatrix} y_1 & x_2 & qy_2 & x_e \end{bmatrix}^\top \\ &= -K_e \begin{bmatrix} x^\top & x_e \end{bmatrix}^\top - k_{e,1} e, \end{aligned} \tag{8}$$

where $K_e \in \mathbb{R}^{1\times 4}$. Then the closed-loop dynamics is

$$\begin{bmatrix} \dot{x} \\ \dot{x}_e \end{bmatrix} = (A_e - B_e K_e) \begin{bmatrix} x \\ x_e \end{bmatrix} - B_e k_{e,1} e,$$

and the equilibrium is

$$(A_e - B_e K_e)^{-1} B_e k_{e,1} e = \begin{bmatrix} 0 & 0 & 0 & -\frac{k_{e,1}}{k_{e,4}} \end{bmatrix}^\top e.$$

Thus, the state x converges to zero, while the integral action x_e ensures the equilibrium offset compensation.

However, to implement the control law (8), it is required to estimate the velocity ω_b. In the next section we discuss possible velocity observers for the considered system.

IV. OBSERVERS DESIGN

A model-based nonlinear observer has been recently proposed in [9] for a class of mechanical systems that are partially linearizable via coordinate changes (PLvCC). The observer can be applied to the mechanical system (2) if it admits a change of coordinates allowing to rewrite the system in such a form that the dynamics is linear in momenta. Then a globally converging exponential momenta observer can be constructed that yields velocity estimation. Unfortunately, despite its simplicity, the considered system does not belong to this class; this claim is rigorously proven in the Appendix .

In this section, we present three designs that are suitable for the considered system, namely a linear model-free differentiator, a linear time-varying observer, and a nonlinear model-based differentiator. The model-free linear differentiator is based on the methods of linear time-invariant system analysis such as Laplace transformation and frequency-domain analysis. This approach is also known as filtered derivative since it can be seen as a serial connection of the (non-realizable) pure differentiator with a low-pass filter. The second approach is motivated by the observability property analysis for linear time-varying systems and Kalman-Bucy filtering. To apply this approach, the considered nonlinear system is rewritten as a linear time-varying one; thus, the estimation error dynamics is also linear and time-varying. Finally, the third method is the nonlinear velocity estimator motivated by the recent advances on homogeneous systems with finite- and fixed-time convergence; the resulting error dynamics of the observer is nonlinear.

A. A LINEAR DIFFERENTIATOR

The simplest way to get the velocity estimation is to use a linear differentiation; however, it is well known that differentiation can be noisy at high frequencies. To this end, a common engineering practice for the velocity estimation is to use a low pass filter together with the differentiator. This can be used to reduce the consequences of noise in the signal but care is needed to ensure that the phase lag does not distort the results. For a 2nd order filter with a time constant τ, the continuous-time transfer function of the model-free differentiator can be written as $G(s) = \frac{s}{(\tau s+1)^2}$, yielding the following state-space realization

$$\begin{aligned} \dot{z}_1 &= z_2, \\ \dot{z}_2 &= -\frac{1}{\tau^2} z_1 - \frac{2}{\tau} z_2 + \frac{1}{\tau^2} y_1, \\ \hat{x}_2^{ld} &= z_2, \end{aligned} \tag{9}$$

where $\hat{x}_2^{ld}$ is the estimate of x_2 provided by the differentiator.

B. A FULL-ORDER LINEAR TIME-VARYING OBSERVER

One classic solution for linear time-varying systems is to construct a linear time-varying observer in the

form

$$\dot{\hat{x}} = \underbrace{\begin{bmatrix} 0 & 1 & 0 \\ 0 & -\dfrac{uJ_2 \sin(2\, y_2)}{J_1 + J_2 \sin^2 y_2} & 0 \\ 0 & 0 & 0 \end{bmatrix}}_{:=A'(y,u)} \hat{x} + \begin{bmatrix} 0 \\ uJ_d\omega_d \cos y_2 + \dfrac{mgl}{\sqrt{2}} \sin y_1 \\ \hline J_1 + J_2 \sin^2 y_2 \\ u \end{bmatrix} - HC^\top (C\hat{x} - y),$$
$$\hat{x}_2^{lo} = \hat{x}_2, \tag{10}$$

where $\hat{x}_2^{lo}$ is the estimate of x_2 provided by the linear observer, the vector of measurements y is defined in (5), $C = \begin{bmatrix} 1 & 0 & 0 \\ 0 & 0 & 1 \end{bmatrix}$ and the time-varying symmetric gain matrix $H(t) \in \mathbb{R}^{3\times 3}$ is the solution of the matrix differential equation

$$\dot{H} = HA'^\top + A'H - HC^\top CH + Q$$

for some $H(0) = H_0 > 0$, and $Q > 0$ is the design parameter. It is known (see, e.g., [17], [18]) that the observer (10) ensures exponential convergence if the system is uniformly observable, i.e., there exist T_O, δ_1, and δ_2, all positive, such that for all t

$$\delta_1 I_3 \le \int_t^{t+T_O} \Phi^\top(\tau, t) C^\top C \Phi(\tau, t) d\tau \le \delta_2 I_3,$$

where $\Phi(\cdot,\cdot)$ is the state-transition matrix of the linear time-varying system $\dot{x} = A'(y, u)x$. This condition is satisfied for the considered system since the pair (A', C) is observable for all values of u, y_2.

Define the estimation error as $\tilde{x} := x - \hat{x}$. Then in the absence of the bias, i.e., when $e = 0$, the error dynamics becomes $\dot{\tilde{x}} = (A' - LC)\tilde{x}$, where $L(t) := H(t)C^\top$, and the convergence of $\tilde{x}$ to zero is ensured.

For the case $e \neq 0$ we have $y = Cx + \begin{bmatrix} 1 \\ 0 \end{bmatrix} e = Cx + C_e e$ and $\dot{\tilde{x}} = (A' - LC)\tilde{x} - LC_e e$. Thus, for observable system the equilibrium differs from the origin $\tilde{x} = 0$ due to the bias e. However, it does not compromise the closed-loop stabilization. Indeed, with the observer, the control action (8) becomes $u = -K_e \begin{bmatrix} \hat{x}^\top & x_e \end{bmatrix}^\top = -K_e \begin{bmatrix} x^\top & x_e \end{bmatrix}^\top + K_e \begin{bmatrix} \tilde{x}^\top & 0 \end{bmatrix}^\top$.

Define $\bar{x} := \begin{bmatrix} x^\top & x_e \end{bmatrix}^\top$. The closed-loop dynamics obeys

$$\begin{bmatrix} \dot{\bar{x}} \\ \dot{\tilde{x}} \end{bmatrix} = \begin{bmatrix} A_e - B_e K_e & B_e K_e \begin{bmatrix} I_{3\times 3} \\ 0_{1\times 3} \end{bmatrix} \\ 0_{3\times 4} & A' - LC \end{bmatrix} \begin{bmatrix} \bar{x} \\ \tilde{x} \end{bmatrix} + \begin{bmatrix} 0_{4\times 1} \\ LC_e \end{bmatrix} e.$$

Then is straightforward to verify that the equilibrium of the closed-loop system satisfies $x = 0$, i.e., the integral action compensates the offset being used in the loop with the state observer even if the observer provides a biased estimate.

TABLE 2. Controller parameters used in experiments.

Description	Symbol	Value
LQR gains in (8)	K_e	[35, 4, -1, 0.3]
Time constant in (9)	τ	0.02
Observer gains in (10)	H_0	$\mathrm{diag}(1, 1, 1)$
	Q	$\mathrm{diag}(1, 5 \cdot 10^6, 1)$
Parameters in (11)	$[k_1, k_2, \alpha]$	[20, 150, 0.85]

C. HOMOGENEOUS FINITE-TIME DIFFERENTIATOR

Following Perruquetti *et al.* [19], the model-based homogeneous differentiator for the states x_1, x_2 of the system (4) is constructed as

$$\begin{aligned} \dot{\hat{x}}_1 &= \hat{x}_2 - k_1 \lceil e_b \rfloor^\alpha, \\ \dot{\hat{x}}_2 &= \frac{u(J_d\omega_d \cos y_2 - J_2 \hat{x}_2 \sin(2y_2)) + \frac{mgl}{\sqrt{2}} \sin y_1}{J_1 + J_2 \sin^2 y_2} - k_2 \lceil e_b \rfloor^{2\alpha - 1}, \\ \hat{x}_2^{hd} &= \hat{x}_2, \end{aligned} \tag{11}$$

where $\hat{x}_2^{hd}$ is the estimate of x_2 provided by the homogeneous observer, $e_b = \hat{x}_1 - y_1$ and $\lceil e_b \rfloor^\alpha = |e_b|^\alpha \operatorname{sign}(e_b)$. In [19] it is shown that if k_1 and k_2 are such that the polynomial $s^2 + k_2 s + k_1$ is Hurwitz and $\alpha \in (\frac{1}{2}, 1]$, then the estimation error $\hat{x} - x$ converges to a vicinity of the origin. More precisely, convergence to the vicinity instead of the finite-time convergence to the origin follows from the replacement of x_2 and $\sin(x_1)$ in $f_2(x, u)$ in (4) with $\hat{x}_2$ and $\sin(y_1) = \sin(x_1 + e)$, respectively. A more detailed analysis of the size of this vicinity can be performed by the means of Lyapunov function analysis in a similar way as in [20]; however, such a result is rather technical and is not presented here for brevity.

V. EXPERIMENTS AND COMPARISON

As we have already mentioned, even if our assumptions allow us to analyze the 1D pendulum, all the experiments presented in this section are performed on the scissored pair.[2] The hardware for the tests (shown in Fig. 2) is assembled from off-the-shelf components. The hardware parameters are summarized in the Table 1. A STM32F746 discovery board was chosen as the main computing unit. We have chosen small brushless motors to drive the wheels D^1 and D^2, the gimbals C^1 and C^2 are actuated by Dynamixel MX106-R servo motors. We use two accelerometers to measure y_1 as it was proposed in [8], and we have installed a fiber optic gyroscope to have the ground truth while comparing the soft sensors that estimate the signal x_2.

To compare the considered estimators on the stabilization task, we first tune the gains of the estimators to have comparable open-loop performance. To this end, we utilize the velocity measurement provided by the fiber optic gyroscope and close the loop with the control law (8). Fig. 4(a) provides the angle measurements y_1 and the corresponding control signal u. Note that after two seconds of the experiment an external force was applied for a short period of time. Using the collected data, we have tuned all three soft sensors to fit the best the measured signal x_2; estimated velocities are

[2]The accompagnying video is available here: https://youtu.be/l7o9A0getPw.

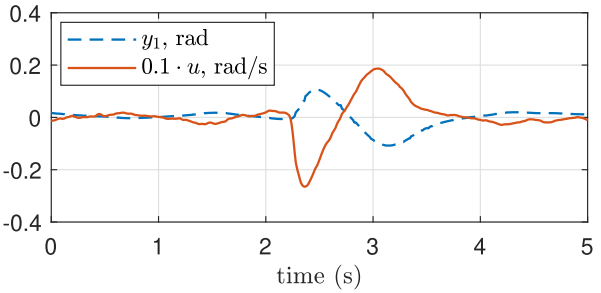

(a) Angle measurement y_1 and corresponding control u

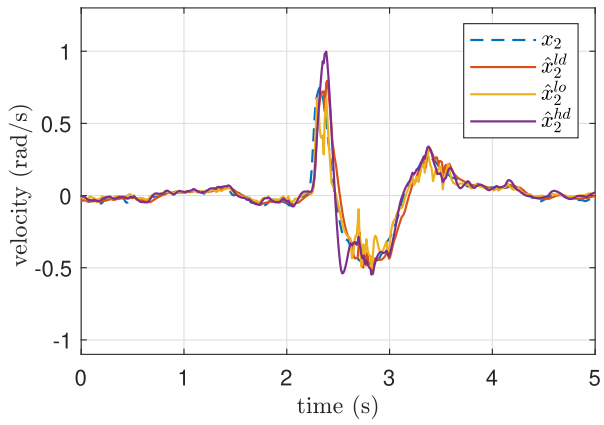

(b) Velocity estimation tuning

FIGURE 4. Observers tuning using ground truth measurements of x_2.

provided in Fig. 4(b). Table 2 summarizes the control gains as well as the parameters of the soft sensors.

At the next step, the previously tuned observers have been compared in the closed-loop stabilization task. To this end, the of fiber optic gyroscope has be disconnected, and the estimate $\hat{x}_2$ provided by soft sensors has been used instead of the signal x_2. The results provided in Fig. 5, 6 and 7 correspond to the velocity estimators (9), (10) and (11), respectively.

The presented experimental results illustrate that the best performance can be obtained using model-based nonlinear differentiator (11). Being model-based, it outperforms the model-free linear differentiator (9), and at the same time it outperforms the model-based linear observer (10). The latter is partially dues to the significant numerical computations required for implementation of the observer (10) as discussed in Remark 1.

Thus, the experimental results support the choice of the model-based nonlinear differentiator (11) as a soft sensor for velocity estimation in the considered application.

Remark 1: It should be emphasized that implementation of the linear time-varying observer (10) in embedded systems is non-trivial; first of all, it is computationally heavy, since the calculation of the gain matrix $H(t)$ requires to solve online several differential equations with quadratic terms that are sensitive to numerical methods. Moreover, for our particular system the gains in the matrix Q (refer to the Table 2) have an asymmetry of six orders of magnitude, thus amplifying the numerical errors.

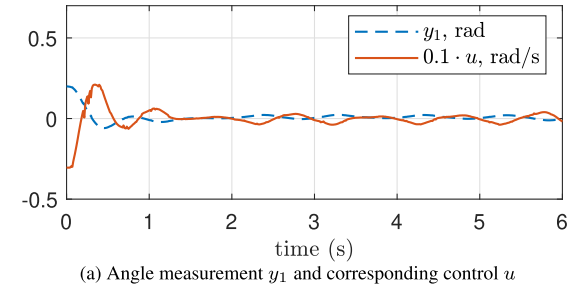

(a) Angle measurement y_1 and corresponding control u

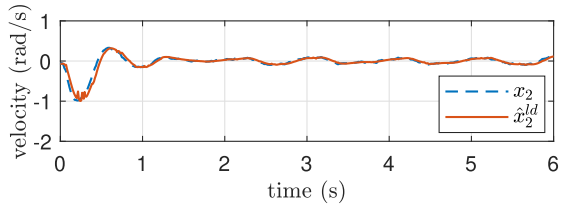

(b) Velocity estimation

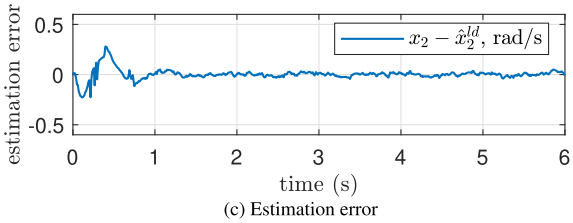

(c) Estimation error

FIGURE 5. Closed-loop stabilization using observer (9).

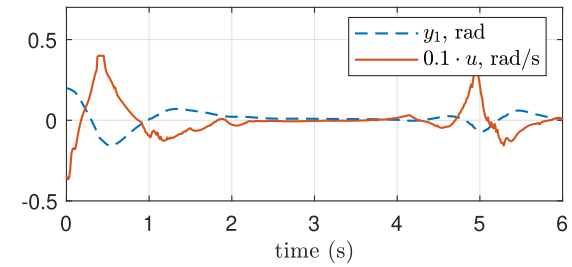

(a) Angle measurement y_1 and corresponding control u

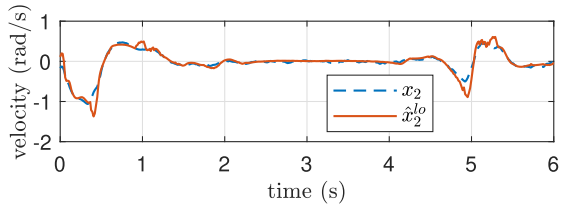

(b) Velocity estimation

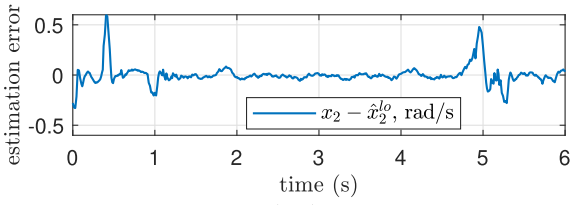

(c) Estimation error

FIGURE 6. Closed-loop stabilization using observer (10).

Note that we have tried to implement a linear time-invariant observer (it can be seen as a particular case of the observer (10)), but we failed to achieve the stabilization, thus we are not reporting these experimental results here.

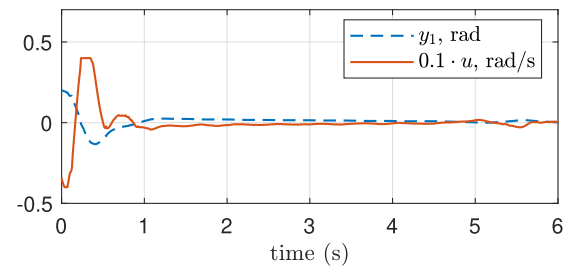

(a) Angle measurement y_1 and corresponding control u

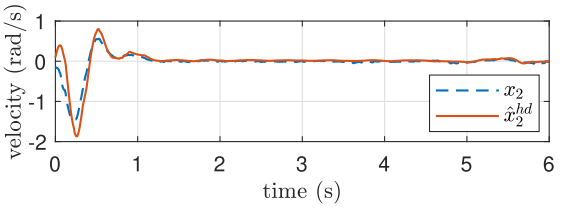

(b) Velocity estimation

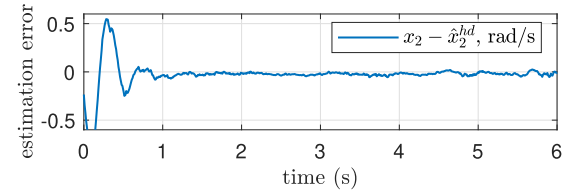

(c) Estimation error

FIGURE 7. Closed-loop stabilization using observer (11).

VI. CONCLUSION

The theoretical results, obtained and confirmed by experimental studies, can be used to stabilize walking biped robots. The developed nonlinear differentiator is able to stabilize the movement of the robot described in the introduction and shown in Fig. 1.

At a further research direction, we intend to apply the designed nonlinear differentiator for the biped system described in Introduction, Fig. 2. At this step, we also intend to incorporate a friction model into the dynamics of the model-based velocity estimator to reduce the modeling errors in the system.

APPENDIX.

In [21] it is proven that a mechanical system with inertia matrix M and n degrees of freedom is partially linearizable via a change of coordinates (PLvCC) if there exists a full-rank matrix $\Psi : \mathbb{R}^n \to \mathbb{R}^{n\times n}$ such that for all $i = 1, \dots, n$ the matrices $\mathcal{B}_{(i)}$ are skew-symmetric, where

$$\mathcal{B}_{(i)} := \sum_{j=1}^{n} \left\{ \left[\Psi_i,\ \Psi_j\right] \Psi_j^\top \left(M\Psi\Psi^\top\right)^{-1} + \frac{1}{2}\Psi_{ji}\Psi \frac{\partial}{\partial q_j}\left(\Psi^\top M \Psi\right)^{-1}\Psi^\top \right\}.$$

Here Ψ_i is the i-th column of Ψ, Ψ_{ij} is the element of Ψ with the indices i and j, and $\left[\Psi_i,\ \Psi_j\right] = \frac{\partial \Psi_j}{\partial q}\Psi_i - \frac{\partial \Psi_i}{\partial q}\Psi_j$ is the Lie bracket.

The system (2) can be written in the standard mechanical system form as $M(q)\ddot{q} + C(q,\dot{q})\dot{q} + G(q) = \tau$, where the inertia matrix is $M(q) = \begin{bmatrix} m_1(q_2) & 0 \\ 0 & 1 \end{bmatrix}$, with $m_1(q_2) := 2\frac{J_1 + J_2\cos^2(q_2)}{I_c + I_d}$. Since the PLvCC property depends on the inertia matrix only, we are not writing down other terms.

In our case we define $\Psi := \begin{bmatrix} a & b \\ c & d \end{bmatrix}$, where a, b, c, and d are the functions of q to be found. Then we obtain

$$[\Psi_1,\ \Psi_2] = \begin{bmatrix} a\frac{\partial b}{\partial q_1} - b\frac{\partial a}{\partial q_1} + c\frac{\partial b}{\partial q_2} - d\frac{\partial a}{\partial q_2} \\ a\frac{\partial d}{\partial q_1} - b\frac{\partial c}{\partial q_1} + c\frac{\partial d}{\partial q_2} - d\frac{\partial c}{\partial q_2} \end{bmatrix},$$
$$[\Psi_2,\ \Psi_1] = -[\Psi_1,\ \Psi_2], [\Psi_1,\ \Psi_1] = [\Psi_2,\ \Psi_2] = 0,$$

To satisfy the PLvCC property, the matrices $\mathcal{B}_{(1)}$ and $\mathcal{B}_{(2)}$ must be skew-symmetric. The equation $\mathcal{B}_{(2)_{2,2}} = -\frac{\partial d}{\partial q_2} = 0$ dictates that d does not depend on q_2, i.e., it is a function of q_1 only. Now let us focus on the following subsystem:

$$\begin{cases} \mathcal{B}_{(2)_{1,1}} = \dfrac{1}{2m_1^2}\left(-2m_1\dfrac{\partial b}{\partial q_1} - d\dfrac{\partial m_1}{\partial q_2}\right) = 0 \\ \mathcal{B}_{(2)_{1,2}} + \mathcal{B}_{(2)_{2,1}} = -\dfrac{1}{m_1}\left(\dfrac{\partial d}{\partial q_1} + m_1\dfrac{\partial b}{\partial q_2}\right) = 0. \end{cases}$$

Since $m_1(q_2) > 0$ for all q_2, we have:

$$\begin{cases} \frac{\partial b(q_1,q_2)}{\partial q_1} = -\dfrac{d(q_1)}{2m_1(q_2)}\dfrac{\partial m_1(q_2)}{\partial q_2} \\ \frac{\partial b(q_1,q_2)}{\partial q_2} = -\dfrac{1}{m_1(q_2)}\dfrac{\partial d(q_1)}{\partial q_1}. \end{cases}$$

The trivial solution is $d = 0$ with $b = b_0$, but it leads to a singular matrix Ψ; let us check if the system has non-trivial solutions. We can differentiate both equations:

$$\begin{cases} \dfrac{\partial}{\partial q_2}\dfrac{\partial}{\partial q_1} b(q_1,q_2) = -\dfrac{d(q_1)}{2}\dfrac{\partial}{\partial q_2}\left(\dfrac{1}{m_1(q_2)}\dfrac{\partial m_1(q_2)}{\partial q_2}\right) \\ \dfrac{\partial}{\partial q_1}\dfrac{\partial}{\partial q_2} b(q_1,q_2) = -\dfrac{1}{m_1(q_2)}\dfrac{\partial^2 d(q_1)}{\partial q_1^2}. \end{cases}$$

The symmetry of second derivatives leads to:

$$\overbrace{-\frac{d(q_1)}{2}}^{\text{depends on } q_1}\ \underbrace{\frac{\partial}{\partial q_2}\left(\frac{1}{m_1(q_2)}\frac{\partial m_1(q_2)}{\partial q_2}\right)}_{\text{depends on } q_2} = \underbrace{-\frac{1}{m_1(q_2)}}_{\text{depends on } q_2}\ \overbrace{\frac{\partial^2 d(q_1)}{\partial q_1^2}}^{\text{depends on } q_1}.$$

Therefore, it leads us to the condition

$$m_1(q_2)\cdot\frac{\partial}{\partial q_2}\left(\frac{1}{m_1(q_2)}\frac{\partial m_1(q_2)}{\partial q_2}\right) = \text{constant}.$$

Since $m_1(q_2)$ is a known function, it is easy to verify that this condition does not hold, and therefore the above system does not admit any (non-trivial) solution. Thus we conclude that this mechanical system is not PLvCC.

REFERENCES

[1] T.-D. Chu and C.-K. Chen, "Design and Implementation of Model Predictive Control for a Gyroscopic Inverted Pendulum," *Appl. Sci.*, vol. 7, no. 12, p. 1272, Dec. 2017.

[2] S. Inc. (Nov. 2019). *Anti-Roll Gyro*. [Online]. Available: https://www.seakeeper.com/technology/

[3] S. D. Lee and S. Jung, "Awakening strategies from a sleeping mode to a balancing mode for a sphere robot," *Int. J. Control Autom. Syst.*, vol. 15, no. 6, pp. 2840–2847, Dec. 2017.

[4] J. Chiu and A. Goswami, "Design of a wearable scissored-pair control moment gyroscope (SP-CMG) for human balance assist," in *Proc. ASME Int. Design Eng. Tech. Conf. Comput. Inf. Eng. Conf.*, Aug. 2014, pp. 1–10.

[5] H. Oya and Y. Fujimoto, "Preliminary experiments for postural control using wearable-CMG," in *Proc. 43rd Annu. Conf. IEEE Ind. Electron. Soc.*, Oct. 2017, pp. 7602–7607.
[6] J. A. Paradiso, "Global steering of single gimballed control moment gyroscopes using a directed search," *J. Guid., Control, Dyn.*, vol. 15, no. 5, pp. 1236–1244, Sep. 1992.
[7] B. Thornton, T. Ura, Y. Nose, and S. Turnock, "Zero-G class underwater robots: Unrestricted attitude control using control moment gyros," *IEEE J. Ocean. Eng.*, vol. 32, no. 3, pp. 565–583, Jul. 2007.
[8] S. Trimpe and R. D'Andrea, "Accelerometer-based tilt estimation of a rigid body with only rotational degrees of freedom," in *Proc. IEEE Int. Conf. Robot. Autom.*, May 2010, pp. 2630–2636.
[9] S. Aranovskiy, R. Ortega, J. G. Romero, and D. Sokolov, "A globally exponentially stable speed observer for a class of mechanical systems: Experimental and simulation comparison with high-gain and sliding mode designs," *Int. J. Control*, vol. 92, no. 7, pp. 1620–1633, Jul. 2019.
[10] L. Ma, G. Zong, X. Zhao, and X. Huo, "Observed-based adaptive finite-time tracking control for a class of nonstrict-feedback nonlinear systems with input saturation," *J. Franklin Inst.*, to be published, doi: 10.1016/j.jfranklin.2019.07.021.
[11] M. W. Spong, P. Corke, and R. Lozano, "Nonlinear control of the Reaction Wheel Pendulum," *Automatica*, vol. 37, no. 11, pp. 1845–1851, Nov. 2001.
[12] A. Levant, "Robust exact differentiation via sliding mode technique," *Automatica*, vol. 34, no. 3, pp. 379–384, Mar. 1998.
[13] L. K. Vasiljevic and H. K. Khalil, "Error bounds in differentiation of noisy signals by high-gain observers," *Syst. Control Lett.*, vol. 57, no. 10, pp. 856–862, Oct. 2008.
[14] W. Perruquetti, T. Floquet, and E. Moulay, "Finite-time observers: Application to secure communication," *IEEE Trans. Autom. Control.*, vol. 53, no. 1, pp. 356–360, Feb. 2008.
[15] D. Sokolov, S. Aranovskiy, A. A. Gusev, and I. Ryadchikov. Nov. 2019. *Experimental Comparison of Velocity Estimators for a Control Moment Gyroscope Inverted Pendulum*. [Online]. Available: https://hal.inria.fr/hal-02313600
[16] ECP (Educational Control Products). (Nov. 2019). *Model 750: Control Moment Gyroscope*. http://www.ecpsystems.com/controls_ctrlgyro.htm
[17] W. J. Rugh, *Linear System Theory*. Upper Saddle River, NJ, USA: Prentice-Hall, 1996.
[18] J. G. Rueda-Escobedo, R. Ushirobira, D. Efimov, and J. A. Moreno, "Gramian-based uniform convergent observer for stable LTV systems with delayed measurements," *Int. J. Control*, vol. 2, pp. 1–12, Jan. 2019.
[19] W. Perruquetti and T. Floquet, "Homogeneous finite time observer for nonlinear systems with linearizable error dynamics," in *Proc. 46th IEEE Conf. Decision Control*, Dec. 2007, pp. 390–395.
[20] I. Ryadchikov, S. Aranovskiy, E. Nikulchev, J. Wang, and D. Sokolov, "Differentiator-based velocity observer with sensor bias estimation: An inverted pendulum case study," *IFAC-PapersOnLine*, vol. 52, no. 16, pp. 436–441, 2019.
[21] A. Venkatraman, R. Ortega, I. Sarras, and A. Van Der Schaft, "Speed observation and position feedback stabilization of partially linearizable mechanical systems," *IEEE Trans. Autom. Control*, vol. 55, no. 5, pp. 1059–1074, May 2010.

STANISLAV ARANOVSKIY (Senior Member, IEEE) received the Engineering, Ph.D., and Dr.Sc. degrees in systems analysis and control from ITMO University, Russia, in 2006, 2009, and 2016, respectively.

He did two Postdoctoral studies at the Umea University, Sweden, and at the Inria Lille, France. In 2014, he joined as a Researcher with the Adaptive and Nonlinear Control Systems Lab, ITMO University. Since 2017, he has been an Associate Professor with CentraleSupélec, campus Rennes, France. His research interests are nonlinear systems modeling and control, estimation and observers design, adaptive systems, and disturbance attenuation. He is a member of IFAC technical committees.

IGOR RYADCHIKOV was born in Krasondar, Russia, in 1985. He received the degree (Hons.) in optical communications engineer from the Faculty of Physics and Technology, Kuban State University. In 2009, he defended his Ph.D. thesis.

In 2014, he created the Laboratory of Robotics and Mechatronics, Kuban State University. In 2017, he established a scientific and educational center World Technologies. The flagship project of the center that receives the support of the Ministry of Science and Higher Education of the Russian Federation is development of control systems for dynamic equilibrium mobile objects. His research team are presented at innovative exhibitions in Singapore, Japan, Great Britain, and Germany.

EVGENY NIKULCHEV was born in Moscow, Russia, in 1975. He received the B.S. and M.S. degrees in control systems engineering from the Moscow State Academy of Engineering Instrument and Information, Moscow, in 1997, and the Ph.D. degree in control engineering, in 2000.

From 2000 to 2006, he was an Assistant Professor with the Department of Modeling and Control Systems, MIREA, Moscow. From 2006 to 2016, he was a Vise-Rector with several Russian universities. Since 2017, he has been a Professor with MIREA–Russian Technological Institute, Moscow. Since 2017, he has also been a Researcher with the Data Center in Russian Academy of Education, Moscow. He is the author of three books and more than 80 articles. His research interests include control systems, identification systems, modeling and simulation, and development of information systems. He is the Chief Editor of the Russian Journal Cloud of Science.

JIAN WANG was born in Zhejiang, China, in 1980. He received the master's degree in computer science and the Ph.D. degree from ITMO University, Russia, in 2006 and 2011, respectively. He is currently an Associate Professor with Hangzhou Dianzi University, China, and ITMO University. His research interests include digital image processing, mode recognition, mobile robot navigation, and nonlinear adaptive control.

DMITRY SOKOLOV received the M.S. degree from Saint Petersburg State University, Russia, in 2003, and the Ph.D. degree in computer graphics from the University of Limoges, France, in 2006.

Since 2008, he has been an Associate Professor with the University of Lorraine. Besides the control theory, his research interest includes digital geometry processing. More specifically, he is interested in parameterization techniques, meshing, and reconstruction of objects from 3D point clouds. These applications include oil exploration, plasma physics, biochemistry, and computer-aided design. He is currently the Head of the PIXEL Research Team, INRIA, French National Research Institute for the Digital Sciences.